Inter-Research Science Publisher

Marine Ecology Progress Series
Volume 779:meps15063

Published February 19, 2026
https://doi.org/10.3354/meps15063

Latitudinal assemblages and vertical distribution of micronektonic crustaceans in the North Atlantic Ocean

Javier Díaz-Pérez[1,*], Juan Ignacio González-Gordillo[2], Santiago Hernández-León[1], Maria José Reyes-Martínez[3], José Maria Landeira[4]

[1]Instituto de Oceanografía y Cambio Global (IOCAG), Universidad de Las Palmas de Gran Canaria, Unidad asociada ULPGC-CSIC, Campus de Taliarte, 35214 Telde, Gran Canaria, Canary Islands, Spain

[2]Instituto Universitario de Investigación Marina (INMAR), Universidad de Cádiz, Campus Universitario de Puerto Real, 11510 Puerto Real, Cádiz, Spain

[3]Universidad Pablo de Olavide, Departamento de Sistemas Físicos, Químicos y Naturales, Ctra. de Utrera, 1, 41013 Sevilla, Spain

[4]Department of Biology, Norwegian University of Science and Technology, Trondhjem Biological Station, 7491 Trondheim, Norway

ABSTRACT: The study of micronektonic organisms in the mesopelagic zone has increased in recent years because of their role in the biological carbon pump. However, most previous studies were focused on fishes, while other significant groups remained unaddressed. Here we analysed the community of micronektonic crustaceans in the North Atlantic Ocean from 20 to 55° N, at different depth layers from the surface to 2000 m depth, and during the day- and nighttime. We identified a total of 111 species belonging to 10 different families of the orders Decapoda, Euphausiacea, and Lophogastrida. Euphausiids were the most abundant organisms (18.3 and 77.0 ind. 1000 m^{-3} during the day and night, respectively), while the Acanthephyridae family (Decapoda) contributed the most to the total biomass (31.9 and 59 g C 1000 m^{-3} during the day and night, respectively). Statistical differences in weighted mean depth showed diel vertical migrants (families Oplophoridae, Pandalidae, Penaeidae, Sergestidae, and Euphausiidae) and families with only some species migrating (Acanthephyridae, Benthesicymidae, Pasiphaeidae, Eucopiidae, and Gnathophausiidae). Based on species composition and abundance, the analyses highlighted 6 different assemblages consistent with existing ecoregions, where temperature and salinity emerged as the primary drivers. Our analysis also revealed connections between the epi- and bathypelagic zones driven by diel vertical migrations. The present study highlights the importance of micronektonic crustaceans in the meso- and bathypelagic zones and calls for more comprehensive research to elucidate their role in the biological carbon pump.

KEY WORDS: Diversity · Diel vertical migration · Mesopelagic · Bathypelagic · Subtropical · Temperate · Decapoda · Euphausiacea · Lophogastrida

1. INTRODUCTION

The world's oceans are undergoing unprecedented changes in temperature, oxygen concentration, and acidity (Hallegraeff 2010), affecting deep-water layers as suggested in recent studies (Santana-Falcón & Séférian 2022, Tjiputra et al. 2023). While some projections predict that pelagic fauna will be severely compromised under current greenhouse emissions (Ariza et al. 2022), others indicate that changes are already detectable in mesopelagic communities (Brodeur et al. 2019, Bograd et al. 2022, Monteiro et al. 2023). In

*Corresponding author: javier.perez@ulpgc.es

Publisher: Inter-Research · www.int-res.com

addition to climate threats, the growing interest of the food and nutraceutical industry in exploiting mesopelagic organisms (Schadeberg et al. 2023) and the potential impact of deep-sea mining (Christiansen et al. 2020, Drazen et al. 2020) must also be considered. As current knowledge of the mesopelagic ecosystem relies mainly on studies of fishes, with micronektonic crustaceans largely overlooked, this ecosystem remains insufficiently explored. The study of deep-water zones is therefore essential to assess the ecosystem services provided by pelagic communities (Martin et al. 2020).

Micronektonic crustaceans are a key component of pelagic food webs (Choy et al. 2016). Their sensitivity to environmental changes can trigger cascading effects throughout the ecosystem (Kelly et al. 2019). These organisms represent a significant portion of standing stocks in the epi-, meso-, and bathypelagic domains (Omori 1975, Vereshchaka et al. 2019). Many species perform diel vertical migrations, remaining at depth during daylight, ascending at night to feed, and descending again before dawn to avoid visual predators. These movements vary widely among and within species depending on size and developmental stage. Some species also exhibit depth-related morphological changes, such as body transparency or the presence of photophores (Vestheim & Kaartvedt 2009). Migratory ranges may extend from the bathypelagic (>1000 m) to the mesopelagic (200–1000 m), or from the mesopelagic to the epipelagic (0–200 m) zone (Vinogradov 1962). Diel vertical migration also transports organic matter to the meso- and bathypelagic zones, contributing to carbon sequestration (Lampitt et al. 2008) on timescales ranging from decades to millennia (Döös et al. 2012). This component of the biological carbon pump has major consequences for ocean biogeochemistry (Archibald et al. 2019). The downward flux of carbon transported by micronekton is highly variable (Hernández-León et al. 2019), and decapods play a particularly important role in this process (Pakhomov et al. 2019).

Euphausiacea, Decapoda, and Lophogastrida are the most abundant micronektonic crustacean taxa. Euphausiids are cosmopolitan diel migrants (Brinton et al. 2000), commonly inhabiting subsurface to mesopelagic layers, although deeper-living forms have also been reported (Angel 1989, Brinton et al. 2000). Among decapods, Acanthephyridae, Sergestidae, Benthesicymidae, and Oplophoridae are most abundant (Vereshchaka et al. 2019). Some species in these families undertake extensive vertical migrations spanning large portions of the water column (Suntsov & Domokos 2013, Bos et al. 2021). Lophogastrids are predominantly deep-living, yet little is known about their distribution or behaviour (Wittmann & Riera 2012, San Vicente 2016, Miranda et al. 2020). Overall, information about micronektonic crustaceans remains limited, particularly regarding their assemblages, behaviour, and contribution to ocean biogeochemistry. Recent barcoding analyses have revealed novel species, thereby enhancing our understanding of interspecific relationships in deep-sea ecosystems (Vereshchaka et al. 2021, 2022). In a previous study, Díaz-Pérez et al. (2024) reported that mesopelagic crustacean communities in the Tropical Atlantic were structured latitudinally, consistent with the ecoregions defined by Sutton et al. (2017). However, high variability in abundance data prevented the identification of specific environmental drivers. The study also characterized the diel vertical migration patterns of several abundant families across the epipelagic and mesopelagic zones, although the analysis was limited by the absence of sampling beyond the mesopelagic layer.

Here, we conducted a latitudinal survey in the North Atlantic Ocean, from subtropical waters off Mauritania to the temperate zone, encompassing the Northwest African upwelling, the oligotrophic waters of the Canary Current, and the productive waters of the North Atlantic. We hypothesized that the ecoregions defined by Sutton et al. (2017) would delineate consistent patterns in the abundance and biomass of epi-, meso-, and bathypelagic crustaceans, corresponding to latitudinal and vertical oceanographic gradients. We further hypothesized that diel vertical migration behaviour would vary along the transect and across the epi-meso-bathy layers in response to regional productivity and hydrographic structure.

2. MATERIALS AND METHODS

2.1. Sampling area

A latitudinal transect was conducted from the oceanic upwelling off Northwest Africa near Mauritania (20° N) to the south of Iceland (55° N), between 24 May and 23 June 2018 (bathypelagic cruise; Fig. 1). The transect crossed multiple mesopelagic ecoregions encompassing distinct water masses. Following Sutton et al. (2017), 4 ecoregions were considered: Mauritania/Cape Verde (MCV), Central North Atlantic (CNA), North Atlantic Drift (NAD), and Northwest Atlantic Subarctic (NAS) (Table 1, Fig. 1).

Each station was sampled for vertical profiles of temperature, salinity, dissolved oxygen, and fluores-

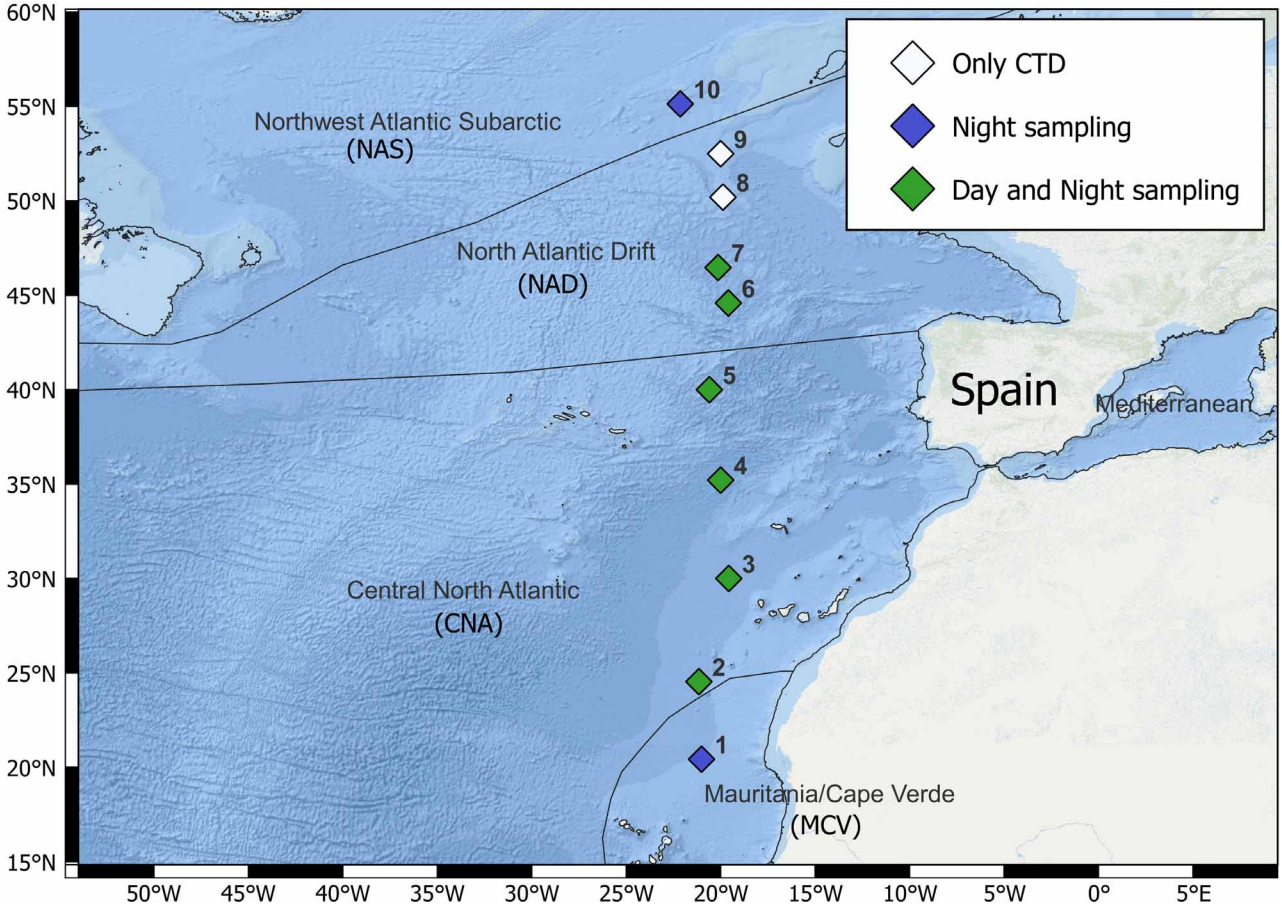

Fig. 1. Location of the sampling stations. Solid black lines delimit the ecoregions given by Sutton et al. (2017). Ecoregions — MCV: Mauritania/Cape Verde; CNA: Central North Atlantic; NAD: North Atlantic Drift; NAS: Northwest Atlantic Subarctic

cence using a Seabird 911Plus CTD profiler equipped with SBE dissolved oxygen and Seapoint chlorophyll fluorometer sensors. Profiles were averaged every 1 dBar and visualized with Ocean Data View software (Schlitzer 2023). Calibration of fluorescence data within the first 200 m to chlorophyll *a* (chl *a*) was based on samples collected at discrete depths with Niskin bottles (see Hernández-León et al. 2019). Vertical sections of oceanographic variables across the transect were generated with Ocean Data View software using the 'DIVA' gridding procedure (Schlitzer 2023).

2.2. Micronekton sampling

Micronekton samples were collected using a Mesopelagos trawl (Meillat 2012) with a single towing cable, a mouth opening of 5 × 7 m, and a total length of 50 m. Mesh size decreased from 30 mm at the mouth to 4 mm at the cod end. The VERDA multi-sampler (Castellón & Olivar 2023) was used to collect samples from 5 layers: 0–200, 200–500, 500–800, 800–1200, and 1200–lowest depth (see Table 1). At Stn 7, the trawl reached 622 m depth, with samples taken in narrower intervals (0–50, 50–100, 100–200, 200–300, 300–400, 400–500, 500–622 m; Table 1). The VERDA device consists of multiple cod ends attached to a revolver mechanism at the end of the net, which rotates at predefined depths to collect samples from distinct layers. Hauls were conducted at 2–3 knots during both day and night, although sampling during both periods was not possible at all stations (see Table 1). The volume of water filtered was estimated from the average mouth area (35 m^2), ship speed, and haul duration. On board, organisms were sorted and preserved in 4% buffered formalin.

2.3. Distribution patterns of pelagic shrimps

In the laboratory, organisms were identified to the lowest possible taxon using standard taxonomic refer-

Table 1. Stations sampled for micronekton indicating the period (D: day; N: night) sampling, number of depth layers, and vertical range sampled for the BATHYPELAGIC oceanographic survey. —: stations where the net could not be deployed. MCV: Mauritania/Cape Verde; CNA: Central North Atlantic; NAD: North Atlantic Drift; NAS: Northwest Atlantic Subarctic (Sutton et al. 2017)

Stn	Period	No. of layers	Vertical range (m)	Ecoregion
1	D	—	—	MCV
1	N	5	0—2024	MCV
2	D	5	0—2033	CNA
2	N	5	0—2252	CNA
3	D	5	0—2071	CNA
3	N	5	0—1844	CNA
4	D	5	0—1772	CNA
4	N	5	0—1881	CNA
5	D	5	0—1817	CNA
5	N	5	0—1750	CNA
6	D	7	0—1852	NAD
6	N	7	0—1899	NAD
7	D	7	0—622	NAD
7	N	7	0—622	NAD
8	D	—	—	NAD
8	N	—	—	NAD
9	D	—	—	NAD
9	N	—	—	NAD
10	D	—	—	NAS
10	N	7	0—1755	NAS

ences (Crosnier & Forest 1973, Casanova 1997, Perez Farfante & Kensley 1997, Brinton et al. 2000, Vereshchaka 2000, 2009, San Vicente 2016). Species names were checked against WoRMS Editorial Board (2023). To obtain wet weight (WW), individuals of the same species in each sample were pooled and weighed. Wet weights were converted to dry weight (DW) using a DW/WW ratio of 0.179 (Pakhomov et al. 2019). Carbon biomass was estimated assuming carbon to be 40% of DW (Olivar et al. 2017, Hernández-León et al. 2019). Abundance and biomass were standardized to the volume of water filtered by the Mesopelagos trawl.

All statistical analyses were conducted in R (v. 4.2.3; R Core Team 2024), using 'ggplot2' (Wickham 2016) for figure plotting and 'vegan' (v. 2.6-4; Oksanen et al. 2022) for statistical analyses. Principal component analysis (PCA) of oceanographic variables was used to classify stations into 4 ecoregions (Fig. 1), which were later applied as factors in subsequent tests. Sampling depth was categorized into epipelagic (0—200 m), upper mesopelagic (200—600 m), deep mesopelagic (600—1000 m), and bathypelagic (>1000 m) layers. Day—night distribution patterns were examined by calculating the weighted mean depth (WMD) at each station for each species, using:

$$\mathrm{WMD} = \sum_{i=1}^{n} P_i Z_i \quad (1)$$

where P_i is the proportion of the taxon in the i^{th} stratum and Z_i is the mid-depth of that stratum. Differences in WMD were tested with ANOVA. When assumptions of normality or homoscedasticity were not met, the non-parametric Kruskal-Wallis test was applied (Fox & Weisberg 2019).

Multivariate analyses were performed in Primer-7 (Clarke & Gorley 2015) on log(x+1)-transformed abundance data to reduce the influence of dominant species. Data were expressed consistently in ind. 1000 m^{-3}, with no further unit conversions. Alternative transformations (e.g. fourth-root) were also tested, yielding similar patterns. Hierarchical clustering was performed using Bray-Curtis similarities, and cluster significance was verified with the SIMPROF test ($p < 0.01$; 999 permutations). SIMPER identified species contributing most to differences among assemblages. Group significance was tested with 1-way permutational multivariate analysis of variance (PERMANOVA) (Anderson 2017), followed by pairwise PERMANOVA to evaluate differences between groups. Finally, canonical correspondence analysis (CCA) was used to assess relationships among species, assemblages, and oceanographic variables.

3. RESULTS

3.1. Oceanographic conditions

We found a broad gradient of temperature along the transect (Fig. 2A). Sea surface temperature ranged from 20°C at 20° N to 10°C at 55° N. Isotherms became shallower towards the north. For instance, the 17.5°C isotherm disappeared north of Stn 5, and similarly the 5°C isotherm occurring at 1500 m depth at 35° N was found at 500 m depth at 55° N. Different water masses were observed along the transect (Fig. 2B). In shallower waters, the Eastern North Atlantic Central Water (ENACW) exhibited salinity values of 37, while the Western North Atlantic Water (WNACW) ranged between 36 and 37 within the first 200 m depth. The Mediterranean Water with a salinity of 36 was detected around 1000 m at 35° N (Liu & Tanhua 2021).

Sea surface oxygen levels (Fig. 2C) remained relatively stable, exhibiting slight variations across stations from the southernmost (225 µmol kg^{-1}) to the northernmost (275 µmol kg^{-1}) stations. However, the oxygen minimum occurred in the 500 m depth layer and exhibited the lowest values (100 µmol kg^{-1}) at 20° N. Northward from this latitude, oxygen levels in-

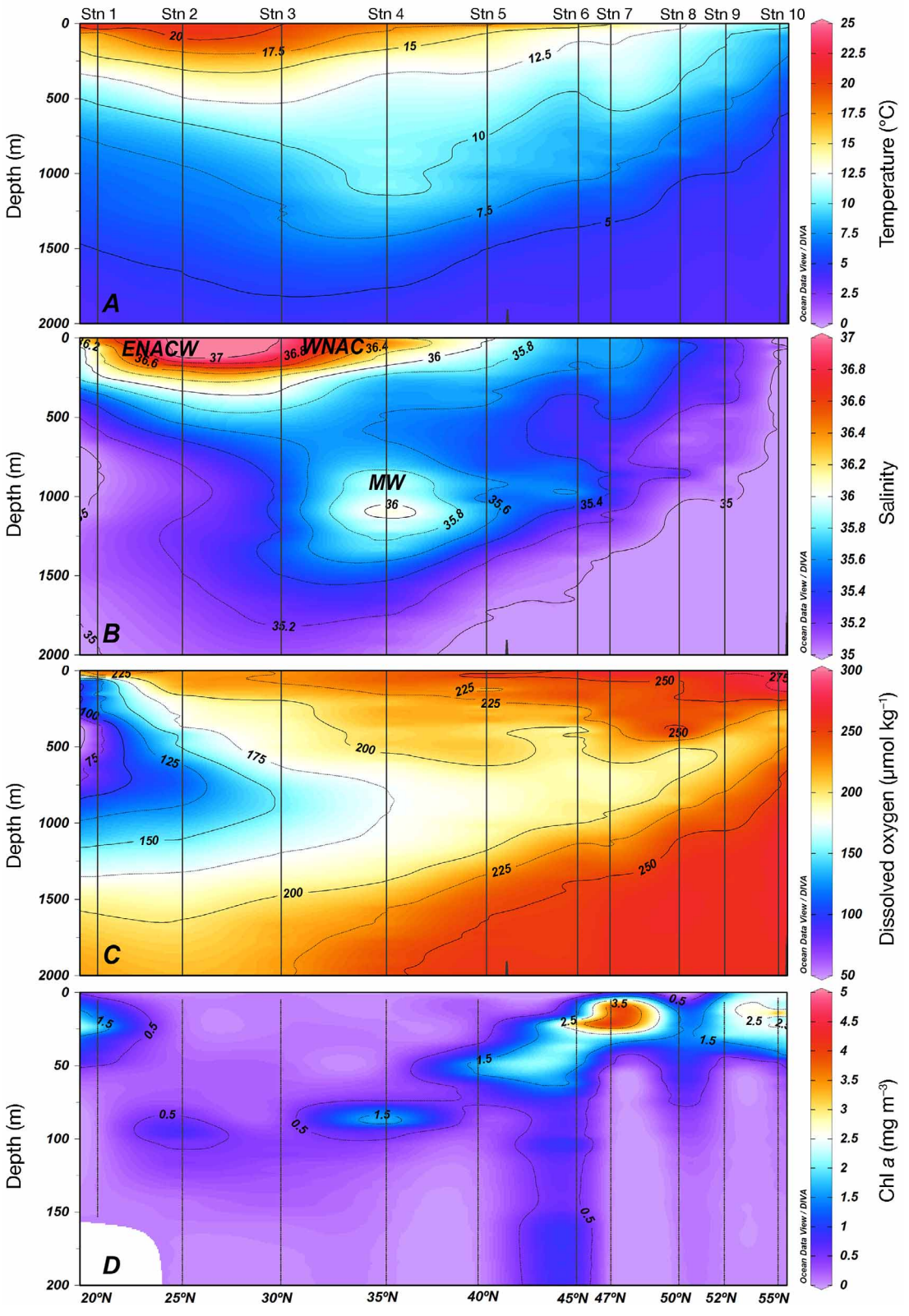

Fig. 2. Vertical section of (A) temperature, (B) salinity, (C) dissolved oxygen, and (D) chl *a* along the BATHYPELAGIC transect. In (B), the water masses detected are shown: East North Atlantic Central Water (ENACW), West North Atlantic Central Water (WNAC), and Mediterranean Water (MW). In (D), the white gap is due to absence of values in that zone. DIVA gridding interpolation was applied for the representation of each variable

creased, reaching 225 µmol kg^{-1} at 55° N. Across the entire transect, chl *a* levels were generally low (Fig. 2D), increasing north of 45° N. The maximum chl *a* value of 3.7 mg m^{-3} was recorded at 47° N (Stn 7) and the second highest value of 2.5 mg m^{-3} at 55° N (Stn 10).

PCA separated the stations according to the ecoregions (Fig. 3, Table 1). Stn 1 differed from the other stations, grouped in MCV with a negative relationship to the oxygen concentration. Stns 2–5 were grouped in CNA stations and showed a positive relationship with temperature and salinity in the whole water column sampled. Stns 6–8 were grouped in NAD and were related to oxygen concentration in the water column. Although Stn 9 belonged to NAD, this station was grouped with Stn 10 in the NAS ecoregion. NAD and NAS groups were positively related to chl *a*.

3.2. Latitudinal distribution of abundance, biomass, and diversity

Integrated values of abundance and biomass (see Table 1 for depths used in calculations) showed a contrasting latitudinal distribution along the transect (Fig. 4). The abundance peak (10.3 ind. m^{-2}) was observed at 20° N (Stn 1) during the night in the oceanic upwelling off Northwest Africa. From this station, values varied between 3 and 5 ind. m^{-2}. Biomass showed its maximum value of 0.33 g C m^{-2} at 40° N (Stn 5), and the second highest value of 0.31 g C m^{-2} was found at 20° N during the night. The latitudinal variation ranged from 0.05 g C m^{-2} at 30° N to the previously mentioned peak at 40° N. For both abundance and biomass, there were no significant differences between day and night samples (Kruskal-Wallis test, $\chi^2_1 = 0.6$, p = 0.812, $\chi^2_1 = 1.06$, p = 0.744, for abundance and biomass, respectively).

Members of the family Acanthephyridae were the main contributors to the total biomass across all the stations (Fig. 5), with values ranging between 50 and 80% of the total. Oplophoridae at Stn 1, and Eucopiidae and Gnathophausiidae at Stn 10 collectively accounted for nearly 40% of the total biomass at each respective station. Abundance at most stations was attributed to Euphausiidae and Acanthephyridae except for Stns 5 and 6, where Eucopiidae dominated the catches, particularly during nighttime.

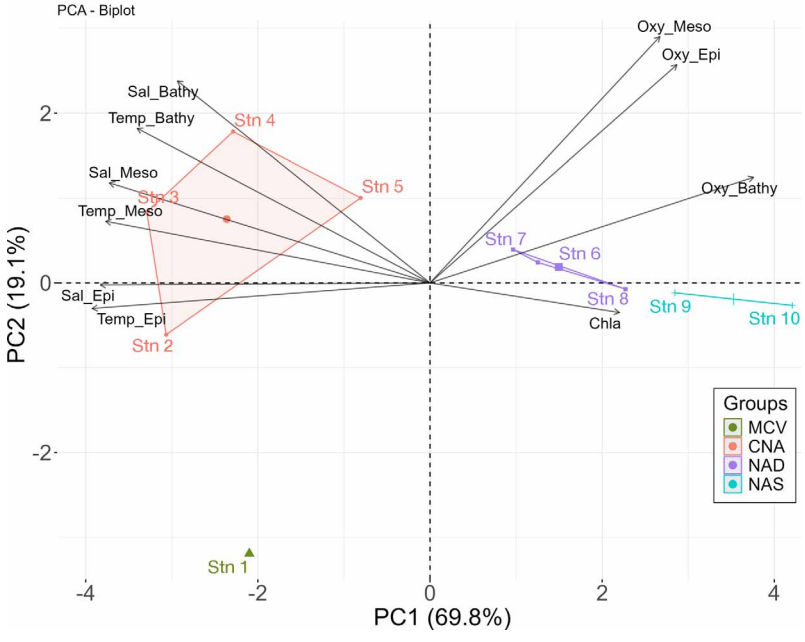

Fig. 3. Principal component (PC) analysis ordination plot of the stations where the net was deployed, shown on the first and second PC axes, which explain 69.8 and 19.1% of the variance, respectively. *K*-means clustering grouped the stations according to the sampled ecoregions. The vectors represent normalized temperature, salinity, oxygen, and chlorophyll *a* (chl *a*) concentrations in the epipelagic (0–200 m), mesopelagic (200–1000 m), and bathypelagic (>1000 m) zones. Note that chl *a* was measured only in the epipelagic zone. Ecoregions — MCV: Mauritania/Cape Verde; CNA: Central North Atlantic; NAD: North Atlantic Drift; NAS: Northwest Atlantic Subarctic (Sutton et al. 2017)

Throughout the transect, we identified 111 species across 10 different families belonging to 3 orders (Table S1 in the Supplement at www.int-res.com/articles/suppl/meps15063_supp.pdf). During nighttime, higher values of both abundance and biomass were observed. The most abundant family was Euphausiidae, comprising 77.0 ind. 1000 m^{-3} of the total abundance during the night, followed by Acanthephyridae with 60.8. In terms of biomass, Acanthephyridae was the predominant family during night- and daytime, accounting for 78.5 and 40.1 g C 1000 m^{-3} of the total biomass, respectively. The contribution of the remaining families was relatively lower. However, families such as Eucopiidae exhibited notable abundance values during both day- (17.5 ind. 1000 m^{-3}) and nighttime (18.0); Oplophoridae also showed a significant contribution during the night (12.6 ind. 1000 m^{-3} for abundance and 10.3 g C 1000 m^{-3} for biomass). At the species level, the major contributor to the total biomass was *Acanthephyra purpurea,* accounting for 19.4 g C 1000 m^{-3} during the day

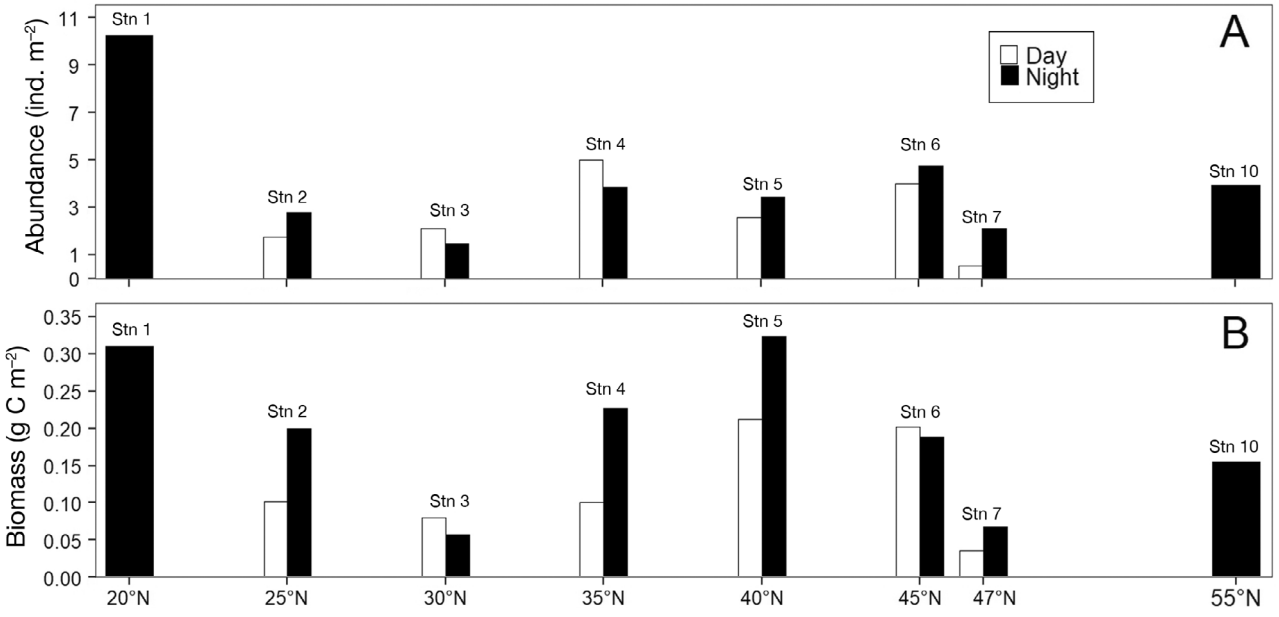

Fig. 4. Latitudinal distribution of integrated values (see Table 1) of (A) total abundance, and (B) total biomass. At Stns 1 and 10, samples were obtained only at night

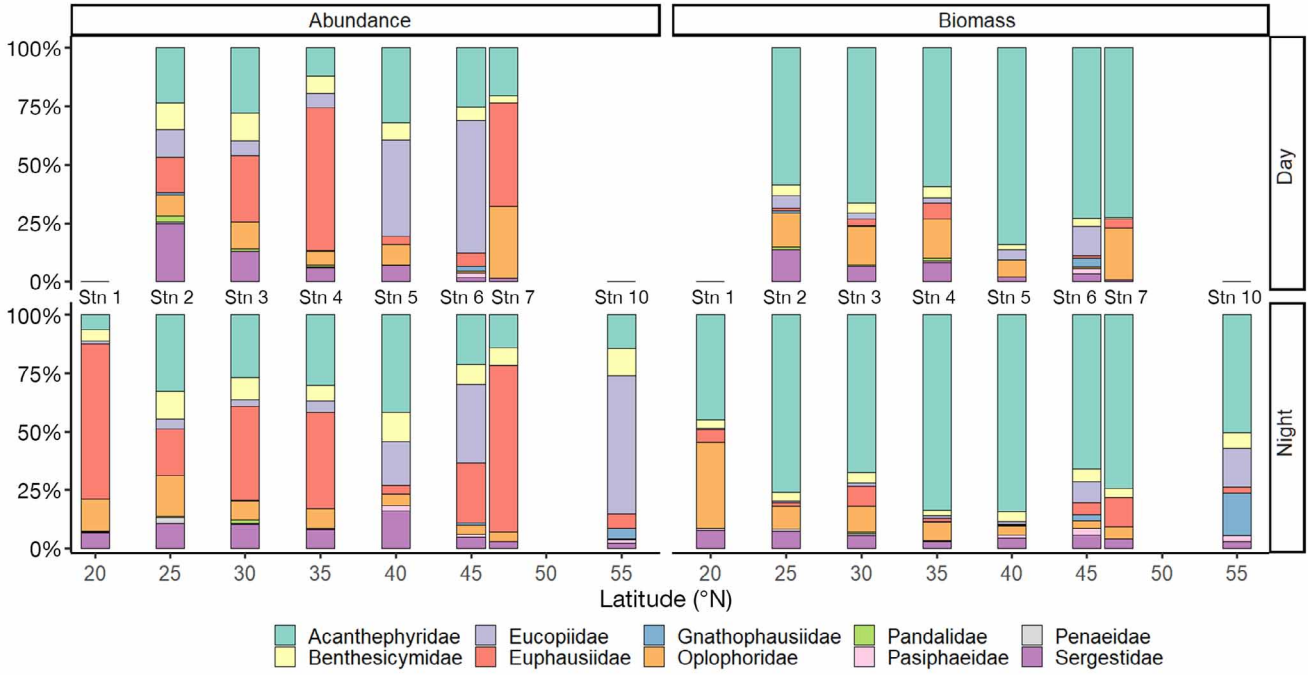

Fig. 5. Percentage of the total abundance and biomass of each family at each latitude during day- and nighttime

and 35.7 g C 1000 m^{-3} at night. In terms of abundance, *Euphausia gibboides* displayed high values of 3.2 and 16.1 ind. 1000^3 m^{-3} during the day and night, respectively. Likewise, *Nematobrachion sexspinosum* was an important species, contributing 2.4 and 13.0 ind. 1000 m^{-3} during the day and night.

3.3. Vertical distribution

We observed patterns of diel vertical distribution at stations where both day and night sampling were performed (Stns 2–7). Overall, during the night an important portion of organisms was collected in the

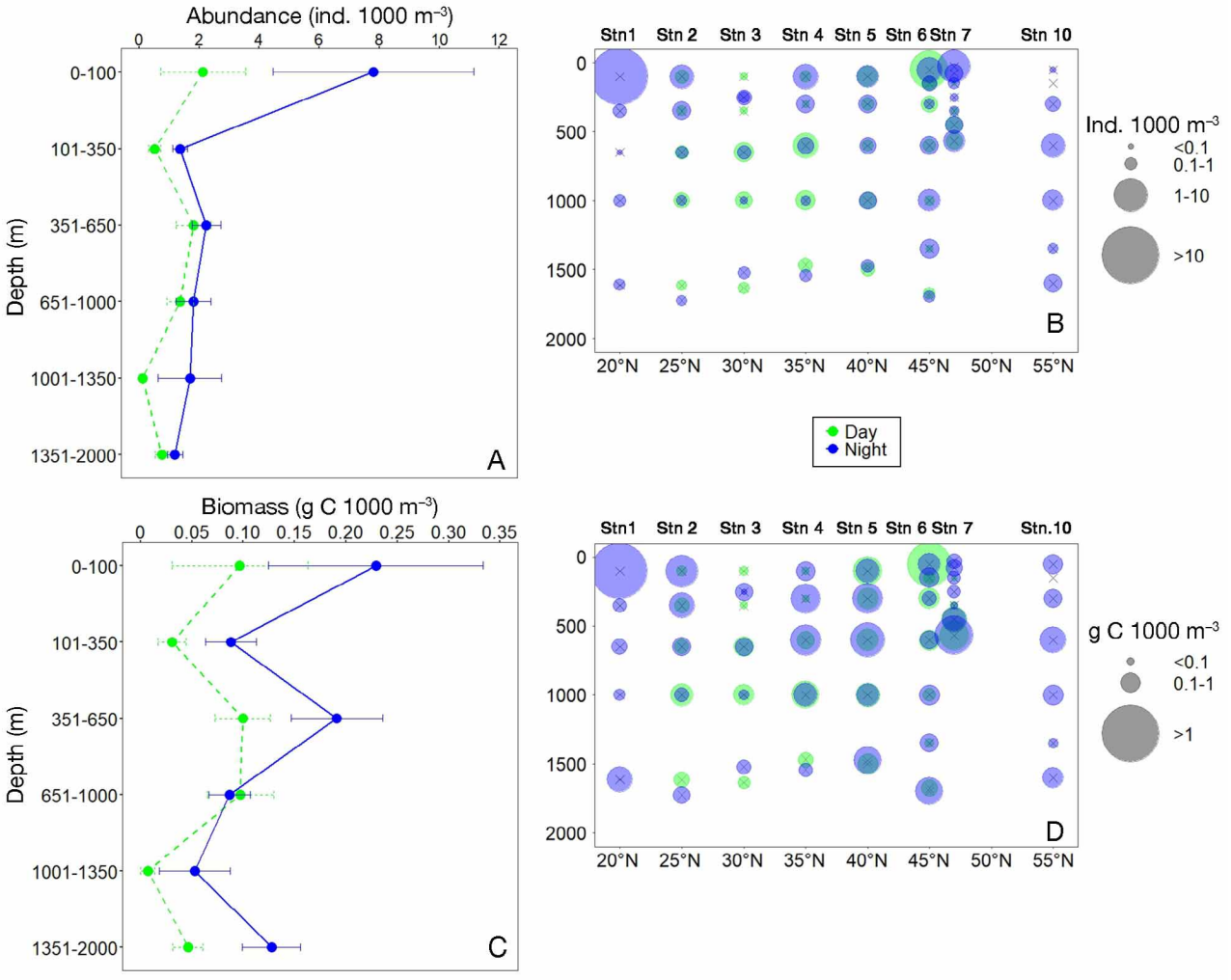

Fig. 6. Vertical distribution of (A,B) abundance and (C,D) biomass during day- and nighttime. (A,C) Average values and standard errors for all stations at each depth layer, and (B,D) values along the latitudinal transect

surface layer (0—100 m) showing abundance values of 7.8 ind. 1000 m^{-3} and biomass values of 0.22 g C 1000 m^{-3}. By contrast, the community was predominantly found in deeper layers (between 350 and 1000 m depth) during daytime (Fig. 6), showing abundance and biomass values close to 2 ind. 1000 m^{-3} and 0.1 g C 1000 m^{-3}, respectively (Fig. 6A,C). However, Stn 6 did not follow this pattern, exhibiting the highest biomass value (0.58 g C 1000 m^{-3}) in the upper 50 m depth during the day (Fig. 6D).

The day—night vertical distribution pattern varied for all identified families. Euphausiidae showed a clear diel vertical distribution, with the highest values near the surface during the night and a shift to deeper layers during the day (Fig. S1A,B; WMD in Table S1). Acanthephyridae showed the same vertical distribution with a slightly more diffuse pattern (Fig. S1C,D). These vertical patterns were statistically validated by comparing the WMD across stations for each family and day- or nighttime (Table 2). This analysis confirmed the vertical migration behaviour for Euphausiidae but the absence of migration for Acanthephyridae. Moreover, the families Pandalidae (Fig. S1G,H), Penaeidae (Fig. S2A,B), and Sergestidae (Fig. S2E,F) were identified as migrants, whereas Oplophoridae (Fig. S1E,F), Benthesicymidae (Fig. S2C,D), Pasiphaeidae (Fig. S2G,H), Eucopiidae (Fig. S3A,B), and Gnathophausiidae (Fig. S3C,D) were considered non-migrants.

3.4. Community structure and assemblages

Cluster analysis showed that the community of micronektonic crustaceans was structured according to depth and ecoregions, displaying 6 groups (SIM-

Table 2. Results of the hypothesis tests for the comparison between weighted mean depth (WMD) and phase for each family. All variables are homoscedastic. The 'Statistic' column reports the test value together with its degrees of freedom, following the format $F_{df1,df2} = ...$ or $\chi^2_{df} = ...$, depending on the test applied

Taxa	Variable type	Hypothesis test	Statistic	p	Behaviour
Acanthephyridae	Normal	ANOVA	$F_{1,14} = 0.010$	0.922	Non-migratory
Oplophoridae	Non-normal	Kruskal-Wallis	$\chi^2_1 = 0.016$	0.897	Non-migratory
Pandalidae	Normal	ANOVA	$F_{1,7} = 18.960$	0.007	Migratory
Penaeidae	Normal	ANOVA	$F_{1,14} = 5.625$	0.098	Migratory
Benthesicymidae	Normal	ANOVA	$F_{1,14} = 0.609$	0.450	Non-migratory
Sergestidae	Normal	ANOVA	$F_{1,14} = 4.623$	0.053	Migratory
Pasiphaeidae	Normal	ANOVA	$F_{1,9} = 0$	0.988	Non-migratory
Eucopiidae	Normal	ANOVA	$F_{1,13} = 0.115$	0.741	Non-migratory
Gnathophausiidae	Normal	ANOVA	$F_{1,10} = 0.433)$	0.433	Non-migratory
Euphausiidae	Non-normal	Kruskal-Wallis	$\chi^2_1 = 4.267$	0.039	Migratory

PROF test 5%, Fig. 7). The groups were identified at a similarity level of 30%. Samples falling below this threshold were not assigned to any group due to their low similarity to other samples, indicating distinct composition. Group A comprised samples from MCV and CNA, characterized by organisms mainly found in epipelagic and upper mesopelagic layers. *Acanthephyra purpurea*, *Systellaspis debilis*, and *Thysanopona*

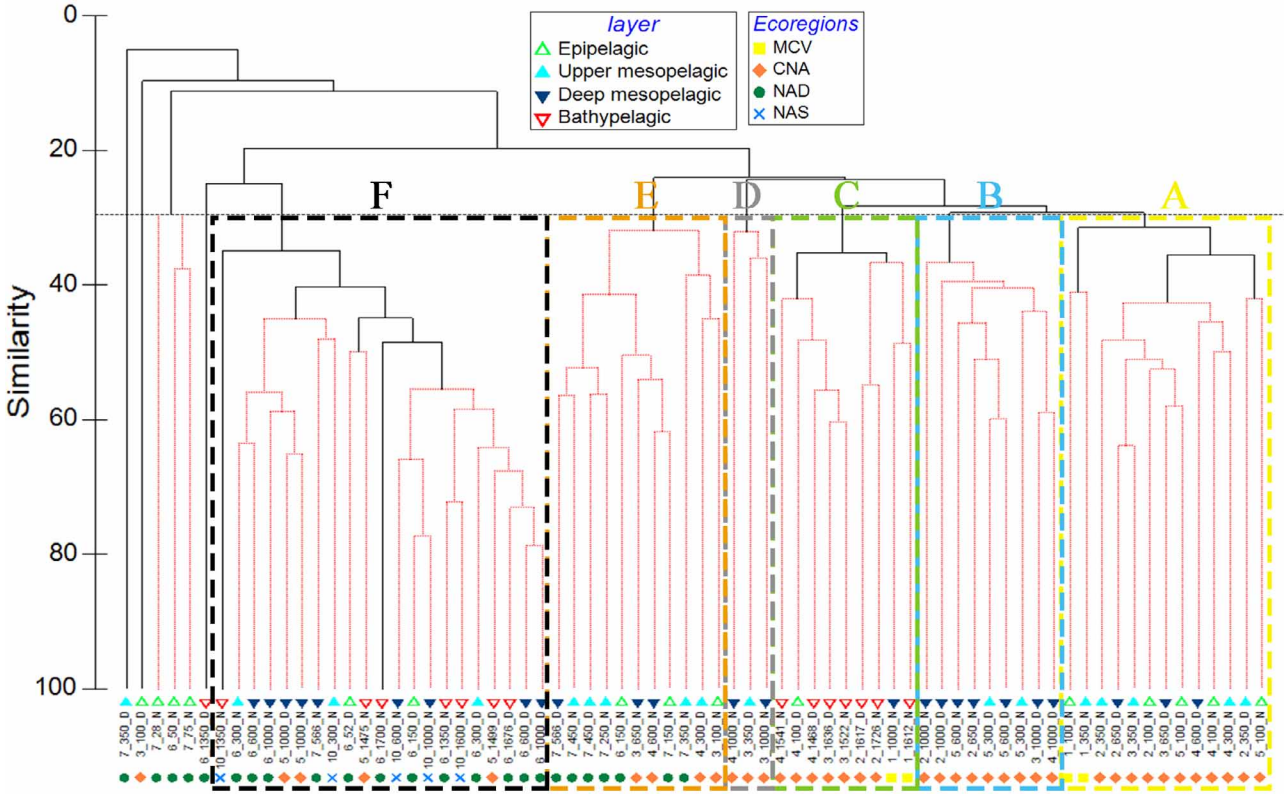

Fig. 7. Hierarchical clustering of station similarities (Bray-Curtis) based on the abundance matrix (log(x+1) transformed). The SIMPROF test identifies clusters that are not significantly different from a random grouping of samples. Red dots in the dendrogram indicate non-significant groupings, meaning there is no statistical evidence to consider these as distinct clusters. The Ecoregion factor represents the 4 regions sampled (Central North Atlantic, CNA; North Atlantic Drift, NAD; Mauritania/Cape Verde, MCV; and North Atlantic Subarctic, NAS) (Sutton et al. 2017). The Layer factor for the 4 depth layers established is also shown (epipelagic: 0–200 m; upper mesopelagic: 200–600 m; deep mesopelagic: 600–1000 m; bathypelagic: >1000 m). Groups are indicated by colours

obtusifrons were the primary contributors to the similarity of the group, accounting for an average similarity of 39.7% (Table 3). By contrast, Group B consisted of samples from CNA with deep mesopelagic organisms, except for 2 samples at Stn 5 associated with the upper mesopelagic zone. The major contributors to the overall similarity in this group were *A. purpurea*, *Eucopia unguiculata*, and *Gennadas valens*, resulting in average similarity of 41.7% (Table 3). Group C was made up of bathypelagic samples from both MCV and CNA stations, including a deep mesopelagic sample and another one from the epipelagic layer. The key species contributing to the similarity within this group were *Bentheogennema intermedia*, *E. unguiculata*, and *Sergia japonica*, resulting in an average similarity of 40.0% (Table 3).

Group D grouped only 2 deep mesopelagic stations and 1 upper mesopelagic station from CNA with an average similarity of 33.4%. Only 4 species achieved at least 90% of the total similarity within this group: *A. purpurea*, *E. unguiculata*, *Gennadas* sp., and *B. intermedia*. Group E represented a mix of samples from epipelagic, upper, and deep mesopelagic layers from CNA and NAD ecoregions. This group had an average similarity of 39.9%, and *Nematobrachion boopis*, *Nematoscelis megalops,* and *A. purpurea* made the most significant contribution to the similarity. Group F consisted mostly of samples collected in deep meso-

Table 3. Species contribution to the similarity for each assemblage obtained in the SIMPER analysis. Average similarity (Sim.) for each group is also shown in parentheses

Group A (Sim. 39.74%)			Group B (Sim. 41.68%)			Group C (Sim. 39.96%)		
Species	Contrib. %	Cum. %	Species	Contrib. %	Cum. %	Species	Contrib. %	Cum. %
Acanthephyra purpurea	16.47	16.47	*Acanthephyra purpurea*	37.34	37.34	*Bentheogennema intermedia*	14.12	14.12
Systellaspis debilis	10.87	27.34	*Eucopia unguiculata*	25.99	63.33	*Eucopia unguiculata*	11.03	25.15
Thysanopoda obtusifrons	8.62	35.95	*Gennadas valens*	15.40	78.73	*Sergia japonica*	9.44	34.59
Gardinerosergia splendens	6.71	42.66	*Sergia japonica*	2.75	81.48	*Acanthephyra purpurea*	8.18	42.78
Eucopia unguiculata	5.15	47.81	*Robustosergia robusta*	2.44	83.92	*Thysanopoda obtusifrons*	6.90	49.68
Euphausia gibboides	5.06	52.87	*Hymenodora glacialis*	2.22	86.14	*Sergia tenuiremis*	5.33	55.01
Nematoscelis megalops	4.31	57.18	*Acanthephyra pelagica*	2.14	88.28	*Hymenodora gracialis*	5.17	60.18
Systellaspis pellucida	4.16	61.34	*Systellaspis cristata*	1.78	90.06	*Gennadas kempi*	5.17	65.35
Oplophorus spinosus	3.57	64.92				*Eucopia grimaldii*	4.81	70.16
Gennadas valens	3.53	68.45				*Eucopia sculpticauda*	3.77	73.93
Nematobrachion boopis	3.27	71.72				*Gardinerosergia splendens*	2.88	76.81
Plesionika richardi	3.16	74.88				*Systellaspis debilis*	2.85	79.66
Robustosergia robusta	2.82	77.70				*Nematoscelis megalops*	2.66	82.31
Deosergestes henseni	2.47	80.16				*Nematobrachion boopis*	2.48	84.80
Sergia tenuiremis	2.38	82.54				*Acanthephyra stylorostratis*	2.19	86.99
Sergia japonica	2.06	84.60				*Meningodora vesca*	1.77	88.76
Systellaspis cristata	1.27	85.87				*Gennadas valens*	1.63	90.39
Thysanopoda monacantha	1.26	87.13						
Bentheuphausia amblyops	0.94	88.08						
Deosergestes corniculum	0.93	89.00						
Eucopia grimaldii	0.92	89.93						
Allosergestes sp.	0.91	90.83						

Group D (Sim. 33.42%)			Group E (Sim. 39.91%)			Group F (Sim. 46.12%)		
Species	Contrib. %	Cum. %	Species	Contrib. %	Cum. %	Species	Contrib. %	Cum. %
Acanthephyra purpurea	75.25	75.25	*Nematobrachion boopis*	34.76	34.76	*Eucopia unguiculata*	22.51	22.51
Eucopia unguiculata	7.08	82.32	*Nematoscelis megalops*	23.50	58.26	*Acanthephyra pelagica*	19.91	42.42
Gennadas sp.	5.72	88.04	*Acanthephyra purpurea*	20.49	78.75	*Eucopia grimaldii*	13.54	55.97
Bentheogennema intermedia	4.29	92.33	*Thysanopoda obtusifrons*	5.46	84.21	*Hymenodora gracialis*	11.34	67.30
			Systellaspis debilis	4.07	88.28	*Gennadas kempi*	8.13	75.43
			Gennadas valens	2.54	90.81	*Bentheuphausia amblyops*	5.30	80.74
						Parapasiphaea sulcatifrons	3.71	84.44
						Acanthephyra purpurea	3.25	87.70
						Sergia japonica	2.65	90.34

pelagic and bathypelagic zones, and a few from epipelagic and upper mesopelagic zones, from CNA, NAD, and NAS ecoregions. This group exhibited a similarity of 46.1%, driven by the contribution of *E. unguiculata*, *A. pelagica,* and *E. grimaldii*. PERMANOVA showed significant differences between groups ($F_{6,75}$ = 9.79, p = 0.001). Those differences were evident in pairwise tests, except between Groups A and D, B and F, C and D, and D and E (Table S2).

CCA (Fig. 8) showed that both temperature and salinity were the environmental drivers that best explained the abundance of the species that most contribute to the formation of each group shown in cluster and SIMPER analyses. Thus, temperature and salinity were correlated negatively with the first axis (−0.87 and −0.81, respectively). In contrast, oxygen showed a lower relationship with both axes (0.51 with the first axis and −0.55 with the second axis). Chl *a* was not related to any axis (0.03 with the first and −0.16 with the second).

4. DISCUSSION

This study encompassed a wide geographic region of the North Atlantic Ocean from 20 to 55° N, and from the epipelagic to the deep bathypelagic zones, showing contrasting oceanographic conditions. Our results provide a snapshot of the micronektonic community of crustaceans, describing their variability in composition and abundance, as well as the vertical distribution patterns during day- and nighttime across a latitudinal transect.

4.1. Methodological constraints

Micronekton sampling is time-consuming on board oceanographic vessels and, together with CTD casts and zooplankton sampling, requires a significant amount of time at each station. However, the Mesopelagos trawl (Meillat 2012) coupled with the multisampler VERDA (Castellón & Olivar 2023) allowed

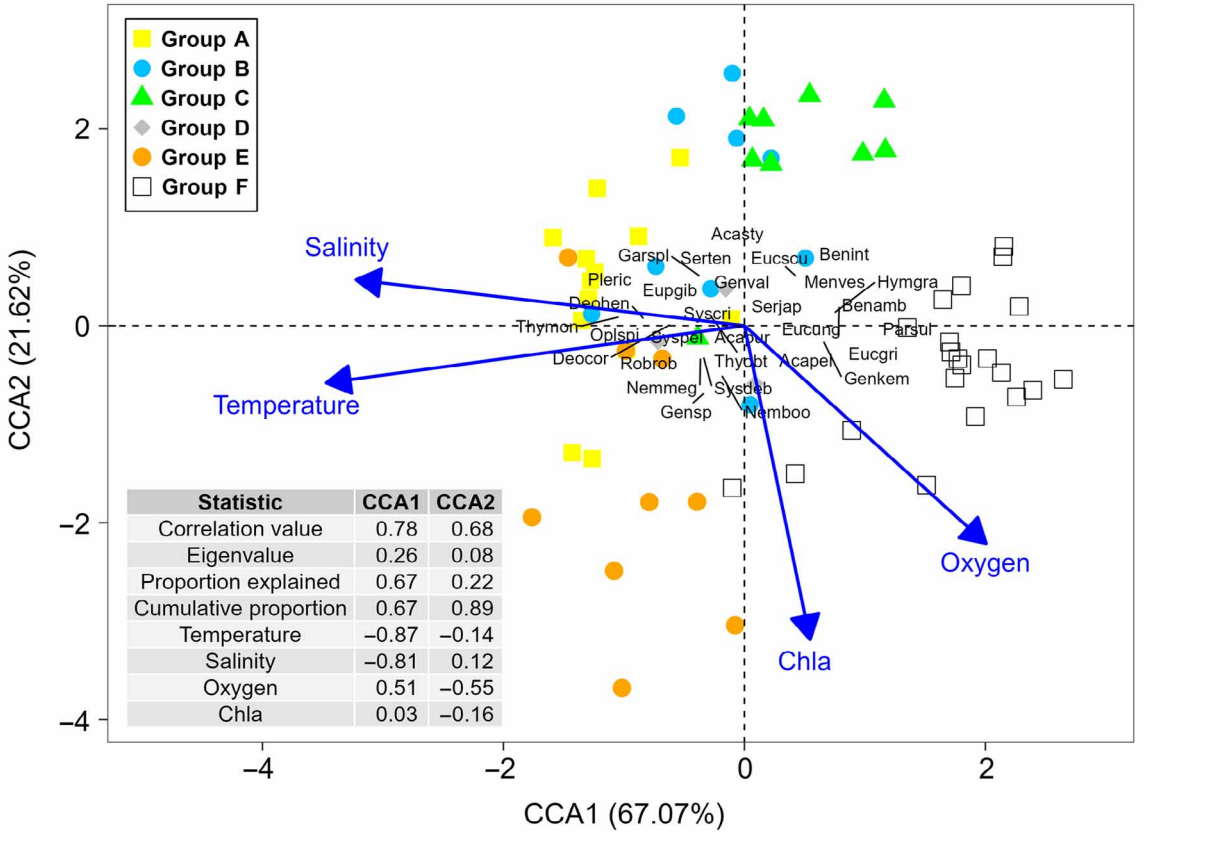

Fig. 8. Canonical correspondence analysis (CCA) with environmental variables (temperature, salinity, oxygen, and chl *a*) and species that most contributed to the formation of each group. Abbreviations of the species name are shown in the figure, and the full name is given in the SIMPER analysis (Table 3). The correlation value of each axis, eigenvalues, the proportion explained, cumulative proportion, and the correlation of each variable with each axis are also shown

stratified samples to be collected at 5 depth ranges in approximately 6 h of trawling, significantly reducing the time required compared with independent trawls at each stratum by traditional pelagic nets. This device also enabled day- and nighttime sampling to explore diel vertical migrations. Nevertheless, differences in trawling strategy (oblique vs. vertical), speed, gear dimensions, and mesh size affect catch efficiency and the ability to capture certain taxa (Pakhomov et al. 2010).

The Mesopelagos net is suitable for sampling a broad range of mesopelagic fish species (Olivar et al. 2017, 2022). Similarly, our results indicate that the net captures a high diversity of micronektonic crustaceans relative to the number of species reported for the North Atlantic Ocean. Thus, 66 decapods were identified from a total of 90 species previously reported (Vereshchaka 2009, Judkins 2014, Vereshchaka et al. 2016), 9 lophogastrids from a total of 16 species (San Vicente 2016), and 21 euphausiids from a total of 47 species reported for the area (Brinton et al. 2000). The relatively low number of euphausiid species found was due to the mesh size of the Mesopelagos net, ranging from 30 mm at the mouth to 4 mm in the cod end. Thus, the net underestimated euphausiids, as adult stages range between 10 and 60 mm (except for larger bathypelagic species such as *Thysanopoda cornuta*) (Brinton et al. 2000). Rare decapods such as *Amphionides reynaudii* and *Psathyrocaris infirma*, previously reported in the North Atlantic Ocean (Landeira & Fransen 2012, De Grave et al. 2015), were not detected. In addition, small and fragile organisms such as *Lucifer typus*, frequently collected in plankton samples (Landeira et al. 2013), were also absent.

One advantage of using the VERDA multi-sampler is that it prevented organisms from being pushed to the bottom of the cod end for an extended period, leading to the recovery of less damaged individuals for identification. Based on our experience, traditional integrated pelagic trawls yield more damaged samples, frequently hindering species-level identifications. This problem is especially pronounced in the case of soft-bodied species such as those belonging to *Gennadas* and *Eucopia*. Moreover, the reduction in mesh size of the Mesopelagos trawl, from 30 mm to 4 mm, appeared adequate for capturing small-sized specimens, as previously observed for small myctophid and stomiiform fishes (Olivar et al. 2017).

For euphausiids, the net configuration allowed sufficient individuals to be caught to describe vertical patterns only for some abundant species. Thus, for this small micronektonic group, the Mesopelagos configuration seemed more suitable than the large pelagic trawls used in the Canary Current by Bordes (2009) and Ariza et al. (2016), which had a mesh size of 80 cm near the trawl opening and decreased to 1 cm in the cod end. However, the IKMT net, fitted with mesh sizes from 0.5 to 10 mm, is likely more suitable for sampling euphausiids (Baker 1970). Nevertheless, the absence of a multi-sampler has the disadvantage of requiring multiple trawls to obtain samples from different depth strata, making operations more time-consuming and inevitably leading to contamination of organisms from upper layers due to integrated samples.

Additionally, horizontal and oblique trawls are less effective at catching pelagic crustaceans than vertical trawls, since, unlike mesopelagic fish, they usually escape by quickly jumping in the vertical direction (Vereshchaka et al. 2019). In fact, the authors reported that vertical trawls resulted in about 24 times higher biomass estimates than other trawling methods. In addition to this lower efficiency, the capture efficiency (CE) of the Mesopelagos trawl is still unknown, and CEs of about 20–50% are commonly assumed for this gear (Hernández-León et al. 2019). Therefore, our catches underestimate the biomass and abundance of micronektonic crustaceans. This issue should be considered when assessing the real ecosystem services (e.g. active flux) provided by micronektonic crustaceans, especially in comparison with other, more extensively studied components such as fish.

4.2. Community assemblages

We identified 6 different assemblages of pelagic shrimps based on composition and abundance across the transect and depth, which could be categorized into 2 latitudinal subdivisions: a southern set (Groups A to D) and a northern set (Groups E and F) (Fig. 7). Under this scenario, we described a gradient of species and assemblages linked to oceanographic conditions. However, establishing statistically significant relationships was particularly challenging due to the high variability in abundance and diversity.

The statistical analyses demonstrated the high significance of the formation of all groups and the differences between them (Fig. 7; Table S1). However, although the SIMPROF test in the cluster analysis showed the significance of the formation of Group D, it did not show significant differences from almost all other groups. This seems to indicate a transition area in the mesopelagic zone where Groups A, B, and E converge, with a gradient of abundance between them.

The southernmost region was represented by Stns 1–5, showing high stratification as expected in the subtropical ocean (Gévaudan et al. 2021). Here, Group A included a combination of epipelagic and upper mesopelagic species typical of tropical and subtropical waters (Table 3, Fig. 8). Group B overlapped vertically with Group A but also included samples from the deep mesopelagic and upper mesopelagic layer of the CNA ecoregion. This group consisted of a limited number of species classified as migrants or deep-dwelling species (Table 3, see Section 4.3) (Burghart et al. 2007, Judkins 2014).

The deepest assemblage within this ecoregion was identified as Group C, characterized by large-range migrant species along with bathypelagic non-migrant species such as *Eucopia* spp., *Bentheogennema intermedia*, *Hymenodora gracilis*, and *Meningodora vesca* (see Section 4.3) (Burghart et al. 2007, Lunina et al. 2024).

Conversely, the northern region (Stns 6–10) displayed a more homogeneous water column structure due to the subsidence of the mixing layer (Dall'Olmo et al. 2016). Group E included samples from both CNA and NAD (Stns 3, 4, 6, 7) and spanned from the epipelagic to the deep mesopelagic layers. This group represented a transition zone between the southern and northern assemblages and coincided with the shoaling of the seasonal thermocline and weak stratification. This was observed in the CCA (Fig. 8), which highlighted temperature and salinity as the main drivers.

Consequently, this area (Group E, CNA–NAD ecoregion) denoted a shift in faunal composition, serving as a transition from the subtropical to the temperate Atlantic Ocean, as proposed by Fasham & Foxton (1979). Stn 7 showed a maximum of 3 mg chl *a* m^{-3} (Fig. 2D), but the CCA revealed no effect on abundance distribution (Fig. 8). This group (Group E) was dominated in terms of abundance by euphausiids, specifically *Nematobrachion boopis* and *Nematoscelis megalops*, which are known to be abundant in the epipelagic and upper mesopelagic layers (Brinton et al. 2000).

The northernmost assemblage, Group F, consisted of samples from deep and cold waters of the CNA, and samples collected in the NAD and NAS ecoregions. A notable feature of this group was the dominance of deep-water crustaceans, including *E. unguiculata*, *E. grimaldii*, *H. gracilis*, and *Bentheuphausia amblyops*, consistent with previous studies of micronektonic crustaceans in cold-temperate waters (MacIsaac et al. 2014). Additionally, there was a shift from *A. purpurea* to *A. pelagica* in the catches, a latitudinal replacement previously documented by Foxton (1972).

In this study, temperature and salinity emerged as the main drivers shaping the abundance of pelagic crustaceans across the transect, consistent with previous findings in the North Atlantic Ocean for decapod species (Foxton 1972, Fasham & Foxton 1979). Examining the relationship between abundance and environmental factors remains essential to anticipate the potential impacts of ocean warming on pelagic crustacean communities.

Migratory behaviour could partly explain how these variables affect different groups, since diel vertical migrants experience broader temperature and salinity ranges by crossing distinct water layers, whereas deep-dwelling non-migratory species remain within narrower ranges (Werner et al. 2012). This might account for the formation of groups observed in Fig. 7, although the metabolic responses to temperature and salinity and the precise tolerance ranges of pelagic crustaceans are still largely unknown. In contrast, oxygen showed little influence on abundance, likely because it was not limiting across most of the transect, dropping below 75 µmol kg^{-1} only near the Cape Blanc upwelling, and because pelagic shrimps exhibit metabolic adaptations to oxygen minimum zones (Childress 1975), complicating any clear relationship with this variable. Similarly, chl *a* showed a weak association with crustacean abundance. Although Vereshchaka et al. (2016) reported linear regressions between chl *a* and decapod wet biomass across depth layers, the correlation coefficients were low, whereas in the same study, zooplankton biomass showed a stronger relationship with chl *a*. This disparity is likely due to decapods, despite their omnivorous habits, showing a preference for zooplankton prey (Omori 1975, Hopkins et al. 1994), an aspect that should be considered in future efforts to predict the abundance or biomass of micronektonic shrimps.

In a previous study, we investigated the latitudinal assemblages of micronektonic crustaceans in the Tropical Atlantic using the same gear and stratified sampling strategy as in the present study (Díaz-Pérez et al. 2024). However, the vertical range of the previous sampling was restricted to 1000 m, while in the present study, the survey extended to 2000 m. This expanded depth coverage was essential for capturing the vertical connectivity between epipelagic migrants and deep-resident assemblages mediated by diel vertical migrations (Fig. 7), a process unresolved in the previous study owing to methodological limitations. Moreover, although Díaz-Pérez et al. (2024) identified latitudinal clusters, they were unable to relate them to specific environmental drivers. In contrast, by integrating a broader depth range and encompassing

subtropical to temperate regions of the North Atlantic, the present study not only corroborates the existence of distinct biogeographic assemblages but also identifies temperature, salinity, and depth as key structuring variables. Therefore, while both studies are complementary, the present work advances beyond descriptive grouping and provides a mechanistic framework linking crustacean community structure to environmental gradients and vertical connectivity within the Biological Carbon Pump.

4.3. Vertical distribution patterns

Vertical migration is a common behaviour among many micronektonic crustaceans (Omori 1975). Nonetheless, the absence of stratified sampling in most studies has limited a more comprehensive understanding of migration patterns at the species level (Foxton 1970). Our sampling strategy and detailed taxonomic identifications enabled the description of fundamental information regarding species behaviour.

Across the transect, statistical analyses determined diel vertical migration at the family level. Nevertheless, analysing the species-level patterns (Table S1) is imperative, since several migrant species were detected within families categorized as non-migrants. For example, at the family level, Oplophoridae did not show migrant distribution patterns, mainly due to the significant variability in the vertical profile observed between 40 and 47° N (Stns 5–7).

The statistical analyses did not show evidence of vertical migration for one of the most abundant oplophorids, *Systellaspis debilis*. Thus, our observations agree with the results reported by Pakhomov et al. (2019) in Hawaiian waters. However, Bos et al. (2021) in the Gulf of Mexico and Foxton (1970) in the Canary Current found strong patterns of vertical migration. This disparity in migratory behaviour may be attributed to factors such as satiation levels, food availability, and size-dependent distribution of the population (Pearre 2003, Bos et al. 2021). The latter factor seems crucial for understanding the behaviour of this species, as Foxton (1970) described ontogenetic migrations, which involves individuals gradually moving to deeper layers as they grow. Foxton (1970) noted that adult individuals, residing in the deep scattering layer during the day, were truly migrating upwards at night, while small juvenile individuals were highly abundant and remained in the upper layers. This size-dependent distribution pattern could mask the signal of vertical migration when combining records from juveniles and adults to estimate abundance. Therefore, future studies should describe the vertical distribution according to the size of individuals.

In our study, the faunal composition of assemblages showed vertical transitions (e.g. between Groups A, B, and C; Fig. 7), which are suggested to be fingerprints of Vinogradov's ladder of migration (Vinogradov 1962), consisting of the connection of the epi- and bathypelagic layers. Such a pattern is exemplified by euphausiids, which played a pivotal role in bridging the gap between epipelagic and mesopelagic layers. Notably, certain species were recorded as bathypelagic organisms (as indicated in Table S1), such as *Meningodora* spp., *Notostomus* spp., and *Hymenodora gracilis* (Angel 1989, Angel & Pugh 2000). For the family Acanthephyridae, *A. purpurea* is a well-known diel vertical migrant moving between the epi- and mesopelagic layers (Foxton 1970). This behaviour explained its high contribution to the characterization of Groups A and B. Finally, the deepest groups (C and F) were characterized by species that could be found in the transition between deep meso- and bathypelagic layers.

The entire process of vertical movements has a significant impact on the functioning of the biological carbon pump. If predator–prey interactions are propagated through Vinogradov's ladder of migration, this mechanism has the potential to transport significant amounts of carbon below the base of the permanent thermocline. There, the carbon could be sequestered for centuries or millennia, on time scales relevant to climate change (Hernández-León et al. 2020). Therefore, the role of micronektonic crustaceans needs to be reconsidered as a core component of the oceanic biological carbon pump and the global carbon cycle.

Data availability. The data sets generated and analysed during the present study are available from the corresponding author upon reasonable request.

Acknowledgements. We thank the crew members and scientists on board the RV 'Sarmiento de Gamboa' and the technicians of the 'Unidad de Tecnología Marina' (UTM) for their support and help during the cruise. This work was funded by projects BATHYPELAGIC (CTM2016-78853-R) and DESAFÍO (PID2020-118118RB-I00) from the Spanish Ministry of Science and Technology, and by SUMMER (Grant Agreement 817806) and TRIATLAS (Grant Agreement 817578) from the European Union (Horizon 2020 Research and Innovation Programme). J.D.-P. was supported by the 'ULPGC2022-2' grant from the Universidad de Las Palmas de Gran Canaria. J.M.L. was supported by the 'Beatriz Galindo' grant (BEAGAL 18/ 00172) from the Spanish Ministry of Science and Innovation.

LITERATURE CITED

Anderson MJ (2017) Permutational multivariate analysis of variance (PERMANOVA). In: Balakrishnan N, Colton T, Everitt B, Piegorsch W, Ruggeri F, Teugels JL (eds) Wiley Statsref: Statistics Reference Online, p 1–15

Angel MV (1989) Vertical profiles of pelagic communities in the vicinity of the Azores Front and their implications to deep ocean ecology. Prog Oceanogr 22:1–46

Angel MV, Pugh PR (2000) Quantification of diel vertical migration by micronektonic taxa in the northeast Atlantic. Hydrobiologia 440:161–179

Archibald KM, Siegel DA, Doney SC (2019) Modelling the impact of zooplankton diel vertical migration on the carbon export flux of the biological pump. Global Biogeochem Cycles 33:181–199

Ariza A, Landeira JM, Escánez A, Wienerroither R and others (2016) Vertical distribution, composition and migratory patterns of acoustic scattering layers in the Canary Islands. J Mar Syst 157:82–91

Ariza A, Lengaigne M, Menkes C, Lebourges-Dhaussy A and others (2022) Global decline of pelagic fauna in a warmer ocean. Nat Clim Change 12:928–934

Baker ADC (1970) The vertical distribution of euphausiids near Fuerteventura, Canary Islands ('Discovery' Sond Cruise, 1965). J Mar Biol Assoc UK 50:301–342

Bograd SJ, Jacox MG, Hazen EL, Lovecchio E and others (2022) Climate change impacts on eastern boundary upwelling systems. Annu Rev Mar Sci 15:303–328

Bordes F (2009) Catálogo de especies meso y batipelágicas: peces, moluscos y crustáceos colectadas con arrastre en las islas Canarias, durante las campañas realizadas a bordo del B/E 'La Bocaina'. Instituto Canario de Ciencias Marinas, Las Palmas

Bos RP, Sutton TT, Frank TM (2021) State of satiation partially regulates the dynamics of vertical migration. Front Mar Sci 8:607228

Brinton E, Ohman MD, Townsend AW, Knight MD, Bridgeman AL (2000) Marine species identification portal: euphausiids of the world ocean. https://euphausiids.linnaeus.naturalis.nl/linnaeus_ng/app/views/introduction/topic.php?id=11&epi=3

Brodeur RD, Auth TD, Phillips AJ (2019) Major shifts in pelagic micronekton and macrozooplankton community structure in an upwelling ecosystem related to an unprecedented marine heatwave. Front Mar Sci 6:212

Burghart SE, Hopkins TL, Torres JJ (2007) The bathypelagic Decapoda, Lophogastrida, and Mysida of the eastern Gulf of Mexico. Mar Biol 152:315–327

Casanova JP (1997) Les mysidacés Lophogastrida (Crustacea) du canal de Mozambique (côte de Madagascar). Zoosystema 19:91–109

Castellón A, Olivar MP (2023) VERDA: a multisampler tool for mesopelagic nets. J Mar Sci Eng 11:72

Childress JJ (1975) The respiratory rates of midwater crustaceans as a function of depth of occurrence and relation to the oxygen minimum layer off southern California. Comp Biochem Physiol A Comp Physiol 50:787–799

Choy CA, Wabnitz CCC, Weijerman M, Woodworth-Jefcoats PA, Polovina JJ (2016) Finding the way to the top: how the composition of oceanic mid-trophic micronekton groups determines apex predator biomass in the central North Pacific. Mar Ecol Prog Ser 549: 9–25

Christiansen B, Denda A, Christiansen S (2020) Potential effects of deep seabed mining on pelagic and benthopelagic biota. Mar Policy 114:103442

Clarke KR, Gorley RN (2015) PRIMER v7: user manual/tutorial. PRIMER-E, Plymouth

Crosnier A, Forest J (1973) Les crevettes profondes de l'Atlantique oriental tropical, Vol XIX (Faune Tropicale). Office de la recherche scientifique et technique outre mer, Paris

Dall'Olmo G, Dingle J, Polimene L, Brewin RJW, Claustre H (2016) Substantial energy input to the mesopelagic ecosystem from the seasonal mixed-layer pump. Nat Geosci 9:820–823

De Grave S, Chan TY, Chu KH, Yang CH, Landeira JM (2015) Phylogenetics reveals the crustacean order Amphionidacea to be larval shrimps (Decapoda: Caridea). Sci Rep 5: 17464

Díaz-Pérez J, Landeira JM, Hernández-León S, Reyes-Martínez MJ, González-Gordillo JI (2024) Distribution patterns of micronektonic crustaceans (Decapoda, Euphausiacea, and Lophogastrida) in the tropical and subtropical Atlantic Ocean. Prog Oceanogr 228:103331

Döös K, Nilsson J, Nycander J, Brodeau L, Ballarotta M (2012) The world ocean thermohaline circulation. J Phys Oceanogr 42:1445–1460

Drazen JC, Smith CR, Gjerde KM, Haddock SHD and others (2020) Midwater ecosystems must be considered when evaluating environmental risks of deep-sea mining. Proc Natl Acad Sci USA 117:17455–17460

Fasham M, Foxton P (1979) Zonal distribution of pelagic Decapoda (Crustacea) in the Eastern North Atlantic and its relation to the physical oceanography. J Exp Mar Biol Ecol 37:225–253

Fox J, Weisberg S (2019) An R companion to applied regression, 3rd edn. Sage, Thousand Oaks, CA

Foxton P (1970) The vertical distribution of pelagic decapods [Crustacea: Natantia] collected on the Sond Cruise 1965 I. The Caridea. J Mar Biol Assoc UK 50:939–960

Foxton P (1972) Observations on the vertical distribution of the genus *Acanthephyra* (Crustacea: Decapoda) in the eastern North Atlantic, with particular reference to species of the '*purpurea*' group. Proc R Soc Edinb 73:301–313

Gévaudan M, Jouanno J, Durand F, Morvan G, Renault L, Samson G (2021) Influence of ocean salinity stratification on the tropical Atlantic Ocean surface. Clim Dyn 57: 321–340

Hallegraeff GM (2010) Ocean climate change, phytoplankton community responses, and harmful algal blooms: a formidable predictive challenge. J Phycol 46:220–235

Hernández-León S, Olivar MP, Fernández de Puelles ML, Bode A and others (2019) Zooplankton and micronekton active flux across the tropical and subtropical Atlantic Ocean. Front Mar Sci 6:535

Hernández-León S, Koppelmann R, Fraile-Nuez E, Bode A and others (2020) Large deep-sea zooplankton biomass mirrors primary production in the global ocean. Nat Commun 11:6048

Hopkins TL, Flock ME, Gartner JV Jr, Torres JJ (1994) Structure and trophic ecology of a low latitude midwater decapod and mysid assemblage. Mar Ecol Prog Ser 109: 143–156

Judkins DC (2014) Geographical distribution of pelagic decapod shrimp in the Atlantic Ocean. Zootaxa 3895:301–345

Kelly TB, Davison PC, Goericke R, Landry MR, Ohman MD, Stukel MR (2019) The importance of mesozooplankton diel vertical migration for sustaining a mesopelagic food web. Front Mar Sci 6:508

Lampitt RS, Achterberg EP, Anderson TR, Hughes JA and others (2008) Ocean fertilization: a potential means of geoengineering? Philos Trans R Soc A 366:3919–3945

Landeira JM, Fransen CHJM (2012) New data on the mesopelagic shrimp community of the Canary Islands region. Crustaceana 85:385–414

Landeira JM, Lozano-Soldevilla F, Hernández-León S (2013) Temporal and alongshore distribution of decapod larvae in the oceanic island of Gran Canaria (NW Africa). J Plankton Res 35:309–322

Liu M, Tanhua T (2021) Water masses in the Atlantic Ocean: characteristics and distributions. Ocean Sci 17:463–486.

Lunina A, Kulagin D, Vereshchaka A (2024) The taxonomic status of *Hymenodora* (Crustacea: Oplophoroidea): morphological and molecular analyses suggest a new family and an undescribed diversity deep in the sea. Zool J Linn Soc 200:336–351

MacIsaac KG, Kenchington TJ, Kenchington ELR, Best M (2014) The summer assemblage of large pelagic crustacea in the Gully submarine canyon: major patterns. Deep Sea Res II 104:51–66

Martin A, Boyd P, Buesseler K, Cetinic I and others (2020) The oceans' twilight zone must be studied now, before it is too late. Nature 580:26–28

Meillat M (2012) Essais du chalut mésopélagos pour le programme MYCTO 3DMAP de l'IRD, à bord du *Marion Dufresne*. (du 10 au 21 août 2012). Rapport de mission, Ifremer

Miranda VR, Vecchione M, Frank TM (2020) Abundance and diversity of deep-sea crustaceans (Decapoda, Lophogastrida, and Euphausiacea) in the micronekton of Bear Seamount, New England Seamount Chain. Mar Biodivers 50: 77

Monteiro M, de Castro SLP, Marques SC, Freitas R, Azeiteiro UM (2023) An emergent threat: marine heatwaves — implications for marine decapod crustacean species — an overview. Environ Res 229:116004

Oksanen J, Simpson G, Blanchet F, Kindt R and others (2022) vegan: Community ecology package. R package version 2.6-4. https://CRAN.R-project.org/package=vegan

Olivar MP, Hulley PA, Castellón A, Emelianov M and others (2017) Mesopelagic fishes across the tropical and equatorial Atlantic: biogeographical and vertical patterns. Prog Oceanogr 151:116–137

Olivar MP, Castellón A, Sabatés A, Sarmiento-Lezcano A and others (2022) Variation in mesopelagic fish community composition and structure between Mediterranean and Atlantic waters around the Iberian Peninsula. Front Mar Sci 9:1028717

Omori M (1975) The biology of pelagic shrimps in the ocean. Adv Mar Biol 12:233–324

Pakhomov EA, Yamamura O, Brodeur RD, Domokos R and others (2010) Report of the advisory panel on micronekton sampling inter-calibration experiment. PICES Sci Rep 38. PICES, Sidney

Pakhomov EA, Podeswa Y, Hunt BPV, Kwong LE, Woodson CB (2019) Vertical distribution and active carbon transport by pelagic decapods in the North Pacific Subtropical Gyre. ICES J Mar Sci 76:702–717

Pearre S (2003) Eat and run? The hunger–satiation hypothesis in vertical migration: history, evidence and consequences. Biol Rev Camb Philos Soc 78:1–79

Perez-Farfante I, Kensley B (1997) Penaeoid and sergestoid shrimps and prawns of the world. Muséum National d'Histoire Naturelle, Paris

R Core Team (2024) R: a language and environment for statistical computing. R Foundation for Statistical Computing, Vienna

San Vicente C (2016) An annotated check-list of lophogastrids (Crustacea: Lophogastrida) from the seas of the Iberian Peninsula. Zootaxa 4178:481–502

Santana-Falcón Y, Séférian R (2022) Climate change impacts the vertical structure of marine ecosystem thermal ranges. Nat Clim Change 12:935–942

Schadeberg A, Kraan M, Groeneveld R, Trilling D, Bush S (2023) Science governs the future of the mesopelagic zone. npj Ocean Sustain 2:2

Schlitzer R (2023) Ocean Data View. https://odv.awi.de

Suntsov A, Domokos R (2013) Vertically migrating micronekton and macrozooplankton communities around Guam and the Northern Mariana Islands. Deep Sea Res I 71:113–129

Sutton TT, Clark MR, Dunn DC, Halpin PN and others (2017) A global biogeographic classification of the mesopelagic zone. Deep Sea Res I 126:85–102

Tjiputra JF, Negrel J, Olsen A (2023) Early detection of anthropogenic climate change signals in the ocean interior. Sci Rep 13:3006

Vereshchaka AL (2000) Revision of the genus *Sergia* (Decapoda: Dendrobranchiata: Sergestidae): taxonomy and distribution. Galathea Rep 18:69–207

Vereshchaka AL (2009) Revision of the genus *Sergestes* (Decapoda: Dendrobranchiata: Sergestidae): taxonomy and distribution. Galathea Rep 22:7–104

Vereshchaka AL, Olesen J, Lunina AA (2016) A phylogeny-based revision of the family Luciferidae (Crustacea: Decapoda). Zool J Linn Soc 178:15–32

Vereshchaka AL, Lunina A, Sutton T (2019) Assessing deep-pelagic shrimp biomass to 3000 m in the Atlantic Ocean and ramifications of upscaled global biomass. Sci Rep 9: 5946

Vereshchaka A, Kulagin D, Lunina A (2021) A new shrimp genus (Crustacea: Decapoda) from the deep Atlantic and an unusual cleaning mechanism of pelagic decapods. Diversity 13:536

Vereshchaka A, Kulagin D, Lunina A (2022) Discovery of a new species provides a deeper insight into taxonomic grouping of the deep-sea genus *Acanthephyra* (Crustacea: Decapoda). Diversity 14:907

Vestheim H, Kaartvedt S (2009) Vertical migration, feeding and colouration in the mesopelagic shrimp *Sergestes arcticus*. J Plankton Res 31:1427–1435

Vinogradov ME (1962) Feeding of the deep-sea zooplankton. Rapp PV Réun Cons Perm Int Explor Mer 153:114–120

Werner T, Huenerlage K, Verheye H, Buchholz F (2012) Thermal constraints on the respiration and excretion rates of krill, *Euphausia hanseni* and *Nematoscelis megalops*, in the northern Benguela upwelling system off Namibia. Afr J Mar Sci 34:391–399

Wickham H (2016) ggplot2: elegant graphics for data analysis. Springer-Verlag, New York, NY

Wittmann KJ, Riera R (2012) Checklist and account of the Lophogastrida (Crustacea, Peracarida) of the Canary Islands, with notes on taxonomy. Rev Acad Canar Cienc 24:63–80

WoRMS Editorial Board (2023) World Register of Marine Species. https://www.marinespecies.org at VLIZ

Editorial responsibility: Marsh Youngbluth, Fort Pierce, Florida, USA
Reviewed by: T. B. Kelly, K. Cook and 1 anonymous referee
Submitted: July 24, 2024; Accepted: November 11, 2025
Proofs received from author(s): February 12, 2026